ELSEVIER

Journal of Chromatography A, 831 (1999) 51–62

JOURNAL OF CHROMATOGRAPHY A

Computer simulation of particle separation based on non-equilibrium swelling

Xiaomi Tong[1], Karin D. Caldwell*

Department of Bioengineering, University of Utah, Salt Lake City, UT 84112, USA

Abstract

Steric/hyperlayer field-flow fractionation (FFF) is an established analytical technique for separating and characterizing particles in the 1–100 μm diameter range. The separation can be based on differences in size, density, shape and mechanical properties of the particles. In the course of an analysis of the water transporter system of Chinese hamster ovary (CHO) cells and one of their high permeability mutants, the first successful attempt was made to use the steric/hyperlayer FFF system for the purpose of separating particles based on a time-dependent property, namely, the differential swelling of the two cell types. The present study was undertaken to simulate numerically the separation in a steric/hyperlayer FFF system of particles with different swelling kinetics. Its purpose was to optimize the separation and suggest selection of operating conditions to minimize repetitive experiments. The computer simulation was developed using Maple V, a symbolic computing environment. It is shown that the model is able to predict an optimal velocity of carrier buffer that maximizes resolution. Predicted velocity/resolution pairs are in good agreement with available experimental data. Empirical models for the lift forces encountered in such FFF experiments, and for the zone broadening observed in work with cell sized particles, form the basis for this model.

Keywords: Computer simulation; Field-flow fractionation; Particle separation; Kinetic studies; Swelling kinetics

1. Introduction

In a recent publication [1] we have described a novel use of the steric/hyperlayer field-flow fractionation (FFF) technique, whereby the separation of two identically sized cells was accomplished by taking advantage of differences in their swelling kinetics when exposed to a carrier of reduced ionic strength. Under normal conditions, Chinese hamster ovary (CHO) cells and their high permeability mutants are not distinguishable by means of their physical characteristics. When they are exposed to hypotonic media, the two cell types swell at different rates due to differences in the water transporter systems of their cell membranes. The cells eventually reach the same size again when the swelling has equilibrated. By taking advantage of the temporary size difference during swelling, the steric/hyperlayer FFF system was able to resolve the two cell types. To our knowledge, this represents the first successful attempt to use an FFF technique for the separation and characterization of particles based on differences in a time-dependent property.

The need for separating or characterizing swellable materials is not limited to cells. For example, in the rapidly advancing drug delivery industry, swell-

*Corresponding author. Present address: Center for Surface Biotechnology, Uppsala University, P.O. Box 577, S-75123 Uppsala, Sweden. Tel.: +46 18 4714000, Fax: +46 18 555016.

[1]Present address: Pasteur Mérieux Connaught, P.O. Box 187, Swiftwater, PA 18370, USA.

0021-9673/99/$ – see front matter
PII: S0021-9673(98)00715-8

able matrices have gained large popularity among pharmaceutical formulators. These materials are used to reduce the dissolution rate of administered drugs in biological fluids [2]. Typical materials used as the swellable matrix are hydrogels and hydrophilic cellulose [3,4] whose swelling can be initiated by changes of salt concentration [4], osmotic pressure [2], temperature [5] or pH [5] in the environment. Since the swelling behavior has a strong relationship to the drug release characteristics of such a matrix, it is important to compare and characterize the swelling behavior of any material to be used for this purpose.

Since the migration velocities of particles in the thin FFF channel reflect both size and density, as well as shape and mechanical properties of the particles, it is reasonable to assume that particles with different swelling rates might be separated and characterized by the FFF technique. The purpose of this study is to develop a model that is able to simulate the elution behavior of swellable particles with already known swelling kinetics, and to find an optimal flow-rate that maximizes the resolution achievable in such a separation.

2. Model of steric/hyperlayer FFF

In order to model the elution behavior in a steric/hyperlayer FFF channel of particles undergoing a time-dependent change in size, it is necessary to first inventory the forces acting on spherical particles of constant size and density, which are subjected to transport by means of a laminar flow through a thin channel under the influence of an externally applied field. These forces will jointly control the particles' equilibrium positions in the parabolic flow profile, and hence their traveling velocities and associated factors which affect resolution in the steric/hyperlayer FFF separation.

2.1. Hydrodynamic lift forces

FFF techniques have performed highly selective separations across the size range of 10^{-3}–10^{2} μm. Submicron particles and polymers are generally separated according to the ''normal mode'' of FFF. By contrast, particles with diameters larger than 1 μm are usually separated by the so called ''steric'' or ''hyperlayer'' mechanisms. The former merely accounts for the fact that large particles are sterically excluded by their very size from the region proximal to the accumulation wall, and therefore incapable of sampling all flow lines in the separation channel. Under the latter mechanism the velocity of particle migration is highly influenced by hydrodynamic lift forces which are not yet fully characterized [6]. The transition of one mechanism into the other is often subtle, and for this reason we prefer to treat them as one and refer to the combination as steric/hyperlayer FFF.

Following injection of sample particles into an FFF channel, the flow of carrier (mobile phase) is normally stopped for a short period of time to allow the particles to be driven to the accumulation wall by the applied field. This stop-flow procedure is called the primary relaxation of the sample, and its purpose is to minimize sample band broadening and premature elution. After this primary relaxation, the carrier flow is initiated to propel the particles through the channel. If the sample consists of large (>1 μm) particles, the presence of a tangential flow will generate flow-dependent hydrodynamic lift forces, which will drive the particles to rise from the accumulation wall and seek a lateral equilibrium position where the lift forces are exactly balanced by the forces exerted on the particles by the applied field. The particles will stay at their respective equilibrium positions if system parameters are kept constant. The process whereby particles reach new equilibrium positions after flow initiation is normally referred to as the secondary relaxation.

The apparent or observed retention ratio R_{obs} is given by the equation:

$$R_{obs} = \frac{t^0}{t_r} = \frac{<v>_{particle}}{<v>_{carrier}} \quad (1)$$

where t^0 is the elution time for non-retained material (void volume), t_r is the elution time of the sample particles, and $<v>_{particle}$ and $<v>_{carrier}$ are the average velocities for sample particles and carrier fluid, respectively. Due to the secondary relaxation effect, R_{obs} will always be smaller than the equilibrium value R_{eq}. However, if the time required for secondary relaxation is short compared to the overall retention time t_r (assumption validated below), the

measured retention ratio R_{obs} will approximately coincide with the equilibrium value R_{eq}. Under constant operating conditions R_{obs} is thus a direct measure of $<v>_{particle}$ and, hence, of the particle's equilibrium position in the parabolic flow profile.

2.2. Empirical lift force studies

In an attempt to quantify the flow-induced hydrodynamic lift forces clearly present in the steric FFF experiment, Williams and co-workers [7–9] studied and modeled the retention behavior of well characterized polystyrene latex microspheres with known size and density. The studies used a wide array of polystyrene latex samples whose retention ratios were measured under varying centrifugal fields and flow-rates.

When particles are transported downstream in the FFF channel at their lateral equilibrium positions, the observed flow-induced hydrodynamic lift force must be equal to the force exerted on these particles by the applied field, as shown in Fig. 1. If a sedimentation field is applied (as in the present study), the field induced force, F_{Field}, is expressed as:

$$F_{Field} = \frac{4}{3}\pi a^3 \Delta\rho G \tag{2}$$

where a is the particle radius, $\Delta\rho$ is the density difference between particle and carrier fluid, and G is the applied sedimentation field.

By assuming identity between this settling force, F_{Field}, and the effective lift force, $F_{Lift,\ eff}$ for particles at their equilibrium position in the channel, Williams was able to develop an empirical equation to predict the magnitude of the lift force acting on a rigid spherical particle with radius a under migration through the thin FFF channel:

$$F_{Lift} = C\frac{a^3 \eta s_0}{\delta} \tag{3}$$

where η is the fluid viscosity, δ is the shortest distance from the particle surface to the channel wall (derived from the observed retention), s_0 is the shear gradient at the wall, and C is a dimensionless coefficient which is system specific. Its value in the described system was determined to be 0.00168, when all parameters in the equation were expressed in cgs units.

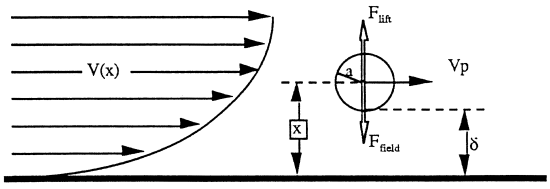

Fig. 1. A spherical particle under migration near a channel wall. F_{Lift} and F_{Field} represent the flow induced lift force and the externally applied field force, respectively. v_p is the elution velocity of the particle, a is the particle radius, while x and δ are the distances between channel wall and particle center of gravity, and between channel wall and particle surface, respectively.

2.3. Retention in the FFF channel

If a rigid spherical particle (radius a) is transported through the flow channel of the FFF system with its center located a distance x from the accumulation wall (so that $x = a + \delta$), its velocity v_p is given by [7]

$$v_p = f(\delta/a)v(x) = 6f(\delta/a) < v > \frac{x}{w}\left(1 - \frac{x}{w}\right) \tag{4}$$

where $v(x)$ is the velocity of the undisturbed fluid at distance x from the accumulation wall, $<v>$ is the average carrier velocity in the channel, and $f(\delta/a)$ is a function whose value equals zero when $\delta/a = 0$ and rapidly approaches unity monotonically as the particle is moving away from the wall. This means that the particle velocity v_p is somewhat less than the undisturbed fluid velocity $v(x)$ at the position of the particle center, a phenomenon referred to as the ''particle retardation effect.'' The numerical values of function $f(\delta/a)$ have been tabulated by Goldman et al. [10].

With the Williams model for the hydrodynamic lift forces acting on spherical latex particles, a particle's elution velocity v_p can be predicted if its size and other separation conditions (namely, flow-rate, field strength, densities of sample and carrier fluid, channel wall thickness, carrier viscosity) are known. By equating the flow-induced hydrodynamic lift force (Eq. (3)) with the force exerted on the particles by the applied field (Eq. (2)), one can calculate δ, and hence a value for x, i.e., the location of the particle center ($x = a + \delta$). Therefore, a particle's elution velocity v_p can be obtained by inserting δ and x into

Eq. (4). Knowing v_p, the particle's retention ratio R can be calculated from the following expression:

$$R = \frac{v_p}{<v>} \quad (5)$$

2.4. Separation resolution and non-equilibrium swelling

The resolution R_s describing an analytical separation of specific components is defined as [11]:

$$R_s = 1.177 \frac{\Delta X}{w'_{1/2} + w''_{1/2}} \quad (6)$$

where ΔX represents the difference in elution volume, or time, between two specified component zones with peak widths at half-height (in volume or time units) amounting to $w'_{1/2}$ and $w''_{1/2}$, respectively.

Estimating $w'_{1/2}$ and $w''_{1/2}$ from a set of chosen experimental conditions is a moderately complex issue, because several factors contribute to zone broadening and their relative effects are unclear. For the purpose of simulating particle behavior in the FFF system used here, we will rely on an empirical model developed from our experimental observations of zone broadening of polystyrene latex particles 6 μm in diameter (shown in Fig. 2). Here, the elution peak width (s) of polystyrene standard particles with a diameter of 6 μm is expressed as a function of average carrier velocity $<v>$. The observed relationship between peak width and velocity for this particle is given by

$$w_{1/2} = 7.148 <v>^{(-0.995)} \quad (7)$$

Simulations based on the above expression for peak width assume that particle size has a negligible effect on this parameter under the focused elution characteristic of hyperlayer FFF.

Thus, for two particles with different size, the separation can be predicted from a combination of Eqs. (3)–(6), with the peak widths given by Eq. (7). Through this approach, the optimal separation conditions can be selected to achieve a desired resolution in separations of a given sample. The strategy is perfectly general and can be applied to any category of separation–characterizations, including those involving particles whose sizes vary with time. In such cases, the particles may have been

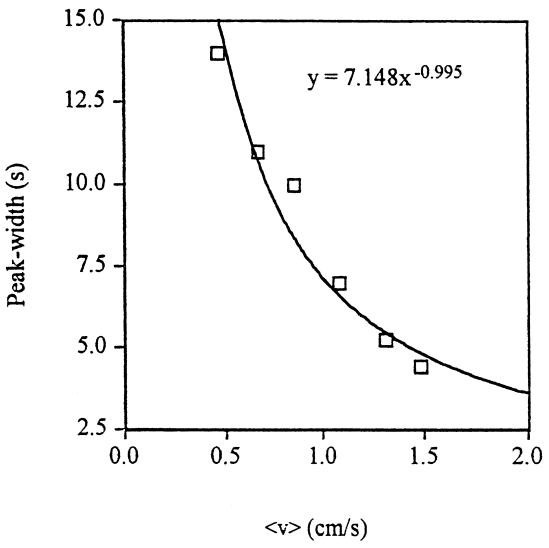

Fig. 2. Peak width (s) as a function of average carrier velocity $<v>$ for standard polystyrene particles with a diameter of 6 μm. Measured widths (cm) from a recorder chart were divided by the selected chart speed (cm/s) to give peak widths (s), in turn plotted vs. average carrier velocity $<v>$ (cm/s).

identically sized under one set of conditions, but may have been induced to swell at different rates as the result of a change in their environment. They may or may not reach the same size again, once their respective swellings have equilibrated. As mentioned above, swellable hydrogels and cells with different membrane permeabilities all fit in this category. Based on a temporary size difference the two particle types may be separated, and their respective swelling kinetics can at least in principle be characterized by the steric/hyperlayer FFF system. To maximize such separations, a numerical simulation is performed to study the effect of separation conditions, in particular the rate of carrier flow, on the resolution of pairs of particles whose sizes vary differentially with time. Thus, unlike in previously described applications of the FFF techniques, neither size, density, nor position in the channel remain constant during the present type of separation and, as a result, the migration velocities for particles undergoing swelling are not constant, but are instead time-dependent. Calculations of particle movements in the channel are therefore significantly more involved than in cases where the particles have constant sizes. For the purpose of predicting resolution in such systems, a

computer program was developed using Maple V (a symbolic computing environment by Waterloo Maple, Waterloo, Canada) to calculate the time-dependent particle velocities v_p, and the resulting time-dependent resolution R_s (parameters defined in Eqs. (4) and (6) above). The empirical lift force model given in Eq. (3) will serve as the basis for predicting the time-dependent particle positions in the channel as functions of the selected shear rates.

3. Experimental

All separation experiments in this study were performed using a sedimentation FFF system built in the laboratory; this system is essentially identical to the Model S-100 from FFFractionation, LLC. The flow channel is 94 cm in length, 2.0 cm in breadth and has a thickness (dimension *w* in Eq. (4)) of 0.0254 cm; the effective void volume of this system is 4.8 ml. Its septum-containing injection port is mounted on the channel wall, and injections, 2–5 μl in volume, were made directly onto the channel by means of a Hamilton micro-syringe. The carrier was delivered to the system by a Rainin Minipuls 3 peristaltic pump; its exact flow-rate was measured by an Ohaus electronic balance. The channel effluent was monitored by a Linear UV detector with a 254 nm light source; its signal was fed to a personal computer, as well as to a chart recorder. In addition to its data collection function, the computer controlled the spin rate of the centrifuge, which was held constant at a field strength of 4 *g* during this study.

Latex particles were from Seradyn, and were analyzed in an aqueous carrier containing 0.1% FL-70 surfactant (Fisher Scientific), while the Chinese hamster ovary (CHO) cells and their Ed-A1 mutants (a gift from Dr. J.F. Ash, University of Utah, UT, USA) were analyzed in phosphate buffered saline of pH 7.4 with ionic strengths varying from 0.15 *M* (normal) to 0.03 *M* (hypotonic).

3.1. Timing of secondary relaxation

The effects of secondary relaxation on particle retention were characterized by a ''delayed relaxation'' method developed in this study (see Fig. 3 for illustration). Standard polystyrene latex beads with a diameter of 6 μm (PS 6 μm) were used for this study. At first, the particles were pumped through the channel at a certain speed without flow stoppage and without applying the sedimentation field. The purpose was to determine the relative velocity of the sample particles ($<v>_{particle}/<v>_{carrier}$) under non-field conditions. Next, after injection of the sample into the channel, a small amount (volume V_f) of carrier fluid was pumped into the channel to transport the sample particles downstream to a new position without applying the sedimentation field. Then, the pump was stopped and the sedimentation field was applied to drive the particles to the accumulation wall. After this delayed primary relaxation the flow was resumed, and the particles transported through the channel in the normal way. The delayed relaxation resulted in a reduction, by volume $V_f(<v>_{particle}/<v>_{carrier})$, of the channel's effective void volume V^0. Each new effective void volume $V^{0\prime}$ can be obtained by:

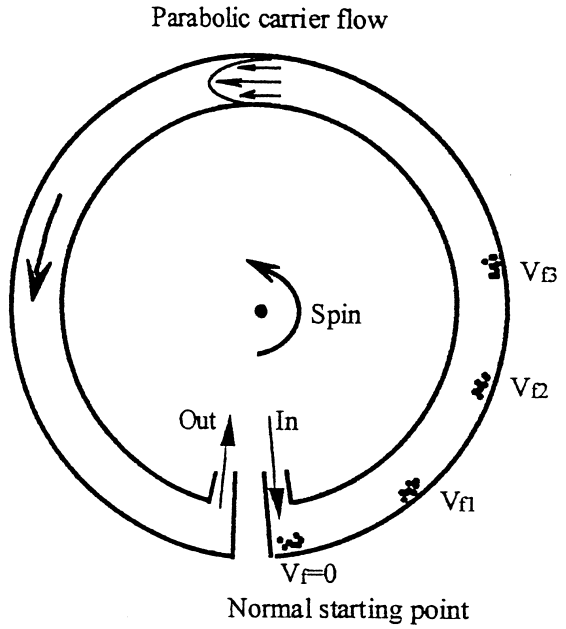

Fig. 3. Characterization of the secondary relaxation effect. Injected samples are relaxed at different locations in the channel, and the effective void volume, i.e., the residual volume in which retention is developed, is used to compute a value for retention ratio *R*. If secondary relaxation is instantaneous, *R* should remain invariant with starting position.

$$V^{0\prime} = V^0 - V_f \frac{<v>_{particle}}{<v>_{carrier}} \quad (8)$$

Since other system parameters were kept constant, the time to achieve secondary relaxation should remain the same for samples at these different starting positions. For shorter effective channel lengths, the relative times for secondary relaxation should be larger compared to the total elution time, and thus the shortfall in R_{obs} should be more significant.

4. Results and discussion

4.1. Characterization of secondary relaxation

The PS 6 μm model particles chosen to examine the rate of secondary relaxation were pumped through the system at a flow-rate of 3.3 ml/min in the absence of a centrifugal field. This carrier flow was moderately high for our experiments, and was chosen to amplify any discrepancies between the expected and observed levels of retention that might be less significant at slower flows. At the chosen flow-rate the ratio $<v>_{particle}/<v>_{carrier}$ was measured to be 1.48, which means that the particle zone actually eluted faster than the average velocity of the carrier fluid. The elution peaks were narrow with a sharp front, indicative of a rapid and complete relaxation into the central flow line. Particles were subsequently injected and allowed to move downstream to different degrees prior to stopping the flow and allowing them to relax under the applied centrifugal field. The amounts of ''over-flow'' generated in this way varied from 0.1 ml to 1.75 ml, and the void volume associated with each new starting position was calculated using Eq. (8). From Fig. 4, it is seen that the observed retention ratios remained constant, even as the effective void volume $V^{0\prime}$ decreased. The standard deviations in these measurements are quite small, as seen in the figure. This result justified our assumption that the effect of secondary relaxation is negligible for particles with sizes comparable to PS 6 μm, and under the typical separation conditions used in this study. In other words, the particles appear to respond instantaneously to changes in the applied lift force.

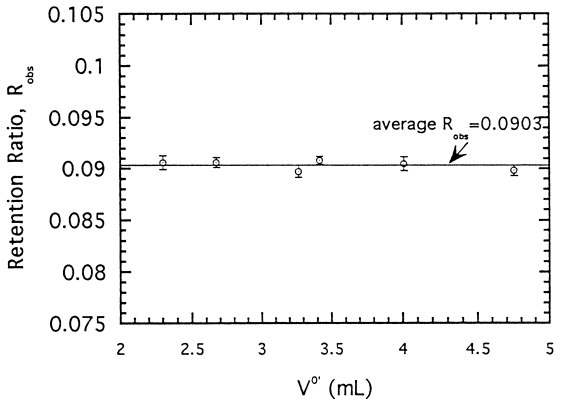

Fig. 4. Observed retention ratios R for sample particles eluting from different starting positions. $V^{0\prime}$ represents the new effective void volume after ''delayed relaxation''. Flow-rate = 3.3 ml/min, field strength = 4 g, relaxation = 15 min.

4.2. Experimental implementation of separation based on differential swelling

A mixture of particles of similar size, but different susceptibility to environmental change, can be separated under conditions of steric/hyperlayer FFF following the strategy outlined in Fig. 5. As suggested by this schematic illustration, the particle mixture is introduced into the channel in a ''normal'' medium and allowed to settle under the influence of the applied field, but in the absence of any channel flow. At the end of this relaxation period flow is resumed, now with a modified medium whose introduction triggers the differential alteration of one or several properties of the sample particles. The efficiency of the ensuing separation will obviously depend on a proper match between the rates of these property changes and the particles' residence time in the channel.

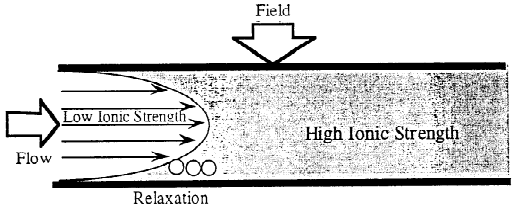

Fig. 5. Experimental arrangement of separations based on differential swelling.

4.3. Development of the model

The structure of the Maple program [12] developed for our simulation study is shown in Fig. 6. If the swelling rates for two particle types are known, the model will be able to compute the resolution for each chosen linear velocity of the carrier buffer, and will thus allow a selection of an optimal flow-rate to achieve the maximal resolution. For that purpose, the operating parameters [namely, field strength G, carrier density, ρ_{buffer}, initial density of the particles, $\rho_p(0)$, channel thickness, w, and carrier viscosity, η] for the separation need to also be input into the model.

To simplify the problem, the particles are assumed to be rigid and spherical. When a particle is swelling, its radius is a function of time: $a(t)$. As the particle increases its size, the influx of buffer will cause a change in particle density; both parameters will influence the settling force induced by the centrifugal field. If $V(0)$, $\rho_p(0)$ and $a(0)$ represent the initial volume, density, and radius of the particle, respectively, $V(t)$ represents the particle volume at time t after initiation of swelling, and ρ_{buffer} represents the density of the carrier buffer, then the time-dependent particle density $\rho_p(t)$ can be expressed as a function of particle radius $a(t)$:

$$\rho_p(t) = \frac{V(0)\rho_p(0) + [V(t) - V(0)]\rho_{buffer}}{V(t)} = \frac{a(0)^3\rho_p(0) + [a(t)^3 - a(0)^3]\rho_{buffer}}{a(t)^3} \quad (9)$$

In addition, as a refinement of the Williams model, the lift force is computed as a function of the local shear rate at the center of the particle, rather than the shear rate at the wall; the local shear rate for undisturbed fluid at distance x ($x = a + \delta$) from the channel wall is given by the following expression:

$$s(t) = \frac{6 < v >}{w}\left(1 - \frac{2[a(t) + \delta(t)]}{w}\right) \quad (10)$$

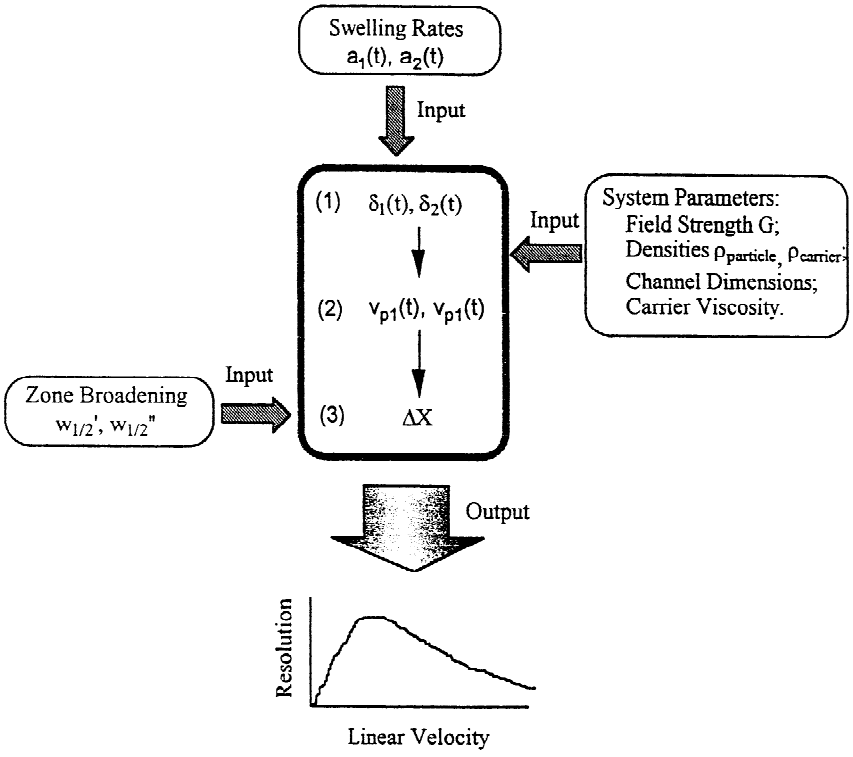

Fig. 6. Structure of the Maple program developed for this simulation study.

The finding of a virtually instantaneous secondary relaxation at the onset of channel flow implies that there is a complete balance between the settling and lift forces acting on a particle at all times. Under two assumptions, namely first, that the modified Eq. (3) (s_0 replaced by s) is a general model for the hydrodynamic lift forces experienced by all types of particles under migration through the FFF channel, and second, that the applied field is a sedimentation field which generates a settling force described by Eq. (2), the following equality is upheld:

$$F_{\text{Field}} = \frac{4}{3}\pi a(t)^3[\rho_p(t) - \rho_{\text{buffer}}]G = F_{\text{Lift}} = C\frac{a(t)\eta s}{\delta(t)} \quad (11)$$

By substituting Eqs. (9) and (10) for $\rho_p(t)$ and $s(t)$, $\delta(t)$ can be expressed as a function of $a(t)$. This is the purpose of the first part of our program, as shown in Fig. 6.

The second part of the program computes particle velocity $v_p(t)$ by inserting $\delta[a(t)]$ into Eq. (4):

$$v_p(t) = 6f\{\delta[a(t)]/a(t)\} < v > \times \frac{a(t) + \delta[a(t)]}{w}\left(1 - \frac{a(t) + \delta[a(t)]}{w}\right) \quad (12)$$

By integrating $v_p(t)$ with respect to time we get an expression for the distance $X(\tau)$ that each particle has traveled in the channel during time (τ):

$$X(\tau) = \int_0^{\tau} V_p(t)\mathrm{d}t \quad (13)$$

Since elution occurs at a distance $X(\tau)$ equal to the known column length, the difference in elution time between two particles, $\Delta\tau$, is easily computed. Thus, for two particle types with different swelling rates, the slower swelling type will have a smaller size than the faster swelling type at any given time, and will travel at a slower velocity through the channel.

To calculate the elution times τ_1, τ_2 and thus $\Delta\tau$ for the two particle types, the above non-linear equation (Eq. (13)) was solved by implementing Newton's method [13] in the computer program. Fig. 7 illustrates this concept. Combining the resulting $\Delta\tau$ with our tentative expression for peak-widths of the two particles in time units allows us to calculate resolution R_s for each given $<v>$, and thereby to select a suitable $<v>$ for the separation problem at hand.

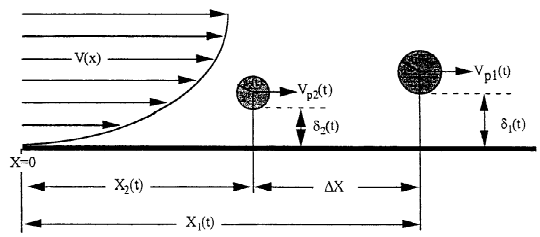

Fig. 7. Migration positions [$X_1(t)$, $X_2(t)$] and velocities $v_{p1}(t)$, $v_{p2}(t)$ for particles of type 1 (fast swelling) and of type 2 (slow swelling).

4.4. Application of the model to a system with known swelling kinetics

Having explained the purpose and the structure of our simulation model, we must ask ourselves: How realistic is this model? Can it be applied to particles with known swelling kinetics? To answer these questions, we will compare the simulation results with our experimental data obtained in our recent study of CHO cells [1].

The swelling rates of CHO cells and their high permeability mutants (''Ed-A1'' cells) in hypotonic medium were discussed earlier; the microscopic observations reported in [1] are reproduced in Fig. 8A. To test our model, we generalize this type of swelling behavior with theoretical swelling rates of two particle types, as shown in Fig. 8B. We define the two types of particles to be separated as having identical sizes under normal conditions, although they swell at different rates once the osmotic environment is changed. When the swelling reaches equilibrium, both particle types will again be of the same size.

The simulated swelling for the two particle types is expressed in terms of changes in their radius, $a_1(t)$ and $a_2(t)$, respectively. Although these theoretical approximations of the real swelling curves are not exact, they describe the observed swelling trends and are therefore considered acceptable for this simulation purpose. As seen in Fig. 8A, the Ed-A1 cells actually begin to shrink after reaching their maximal size. This ''regulatory volume decrease'' is thought

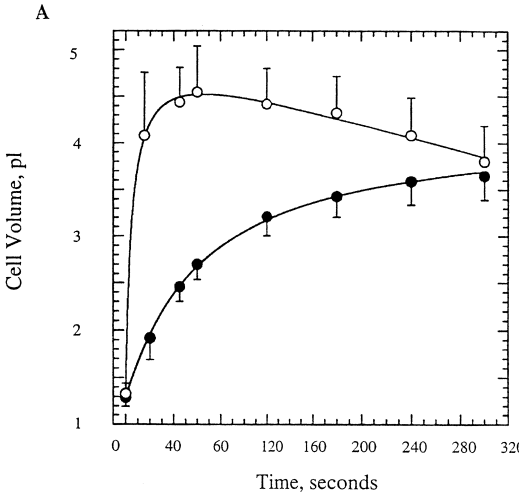

Fig. 8. Differential swelling rates of CHO cells and the Ed-A1 mutant. (A) Microscopic observations of CHO (●) and Ed-A1 (○) cells. (B) Theoretical swelling curves for spherical particles of type 1 (fast swelling) and type 2 (slow swelling) used in this study to test the simulation model.

to be induced by a loss of cytoplasmic amino acids during the initial rapid swelling [14,15]. Since the phenomenon is not fully understood, and not generally applicable to other types of particles, we prefer not to include this volume change in the present model evaluation. Therefore, our assumed swelling kinetics will somewhat underestimate the temporal differences in particle size during a significant portion of the swelling period. Consequently, our model will likely predict smaller than actual values for $\Delta\tau$ and resolution, even from experimental conditions known to cause separation of CHO and Ed-A1 cells. The test of our model is made using the theoretical swelling rates from Fig. 8B, together with a set of operating parameters typical for cell separation in our steric FFF system. The resulting graph of resolution versus average linear velocity of the carrier buffer is shown in Fig. 9. It suggests that at very low carrier velocities (~0 cm/s) the resolution is approximately zero, but increases gradually with increasing carrier velocity until a maximum is reached. For the particular set of conditions tested, the resolution maximum (R_s~2.3) is predicted to be reached at a velocity of ~22 cm/s. If the linear velocity continues to increase, the resolution will again decrease, and will be less than 0.01 when $<v>$ is larger than 1500 cm/s (data point not shown in the graph).

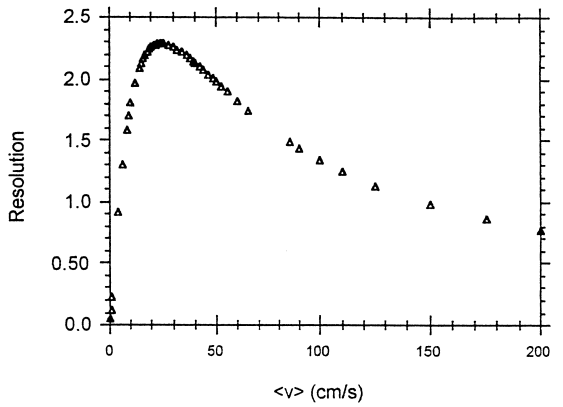

Fig. 9. Resolution vs. average flow-rate, as predicted by the simulation model.

The prediction that the resolution function passes through a maximum with increasing linear velocity is not surprising, since at very slow flow velocities, the particles will spend excessive amounts of time in the channel. From the perspective of their swelling rates, their elution times will be close to infinity. The period of time when the particles differ in size will then be practically negligible compared to τ_1 and τ_2. Before the difference in size can cause any significant difference in the distances traveled, the particles will again have reached the same size (although they are now larger), and hence they will again travel with the same velocity. Therefore, the two particle types are not separable when the carrier velocity is too low, i.e., the resolution is close to zero. On the other hand, when the carrier velocity is very high, the particles will already have been swept through the channel before their sizes have come to differ by a

significant amount. Thus, at very high carrier velocities the resolution will again decrease to zero.

The present model predicts the optimal resolution to be achieved at an average linear velocity of around 22 cm/s, which in our steric FFF system, with its channel cross-sectional area of 0.0508 cm^2, translates into an average volumetric flow of 67.06 ml/min. Such a flow-rate far exceeds the ability of our pumping system, which can only deliver less than 10 ml/min through the channel. In addition to the limited pumping speed of our system, the concern of causing cellular damage under such high shear stress has led us to choose average velocities of less than 2 cm/s in our cell separation experiments.

For the average carrier velocity ($<v>=1$ cm/s) used in our separation of CHO cells and their Ed-A1 mutants [1], our model predicts a resolution of $R_s=$ 0.53. The measured resolution from the fractogram of this separation (Fig. 10) is 0.74. Given the many assumptions incorporated in our model, it is gratifying that the resolution data show this good an agreement. The difference between the measured swelling curves and our simulated model is one likely factor that causes the model to predict a lower resolution than that found experimentally. Even though the simulation results are in reasonable conformity with our experimental observations on CHO cells and their mutants, the retention model upon which they are based has some limitations that will require future improvements.

First of all, the empirical expression for the lift forces experienced by particles under shear stress in the steric/hyperlayer FFF system was developed only for rigid spherical latex particles. As is evident from our studies of red cells [16], the lift forces experienced by deformable particles are greater than those predicted by Eq. (3). Even though most cells are not nearly as deformable as the red cells, their deformabilities are obviously larger than those characteristic of rigid latex particles. In addition, as exemplified by the disc-shaped erythrocytes, cells may not have a perfect spherical shape and may therefore experience lift forces of different magnitude than those used in the model. However, since no perfect model is currently available to describe the lift forces on particles with various shapes, deformabilities and other physical properties, we have accepted the model by Williams and co-workers as the currently best estimate of the lift forces in order to simulate general particle migration behavior in the FFF channel. If a better model is developed in future research for some particle type of interest, that model can be easily substituted into our simulation to replace the current lift force expression.

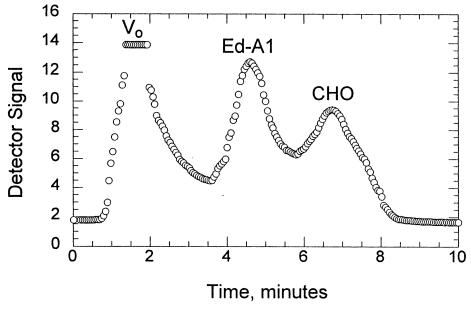

Fig. 10. Actual separation of a mixture of Ed-A1 and CHO cells. The mixture was injected and allowed to settle in a medium of physiological ionic strength, elution with hypotonic medium was initiated at time 0 min. The field strength was 4 *g* and the flow-rate 3.0 ml/min.

Second, as was mentioned above, our expressions for zone broadening in this study are tentative and are based on our experimental observations of polystyrene latex particles. It is highly possible that the zone broadening effects for cells are different than those observed for polystyrene particles. In addition, due to the limitations of the pumps used in our system, no experimental data are available for $<v>$ larger than 3 cm/s. It is unclear whether the empirical expressions used here for zone broadening and lift are still valid for higher carrier velocities. However, our program is constructed in such a way that it can be easily modified if better models are developed to describe zone broadening effects.

5. Conclusions

The FFF techniques are normally utilized to separate macromolecules and particles based on some property that remains constant throughout the analysis. From the present work it is clear that the concept can be expanded to apply also to mixtures of samples which are apparently identical, but which can be temporarily altered in a differential way to allow segregation. The subtechnique employed to

accomplish the separation of interest here is the sedimentation FFF in its steric/hyperlayer mode. This technique is primarily selective to differences in size, but shifts in size lead to shifts in several other interrelated parameters important for resolution, namely density, position in the flow field and zone broadening.

The particle hyperlayer is formed through the focusing influence of two opposing forces due to field induced settling and velocity derived lift, respectively. Of these, the settling force has a well known relationship to size and density, while the lift force can, as yet, not be described from first principles. An empirical model was developed some time ago by Williams and co-workers based on the assumption that the two forces were exactly matched during the entire elution, and that the magnitude of the lift force therefore was identical to the readily calculable settling force. This assumption was clearly validated during the course of the present study.

In order to select proper operating conditions for the timely resolution of a mixture of swellable particles we have undertaken to model the separation process using a modularized algorithm that was implemented in Maple V. The previously developed empirical lift force expression was accepted as one of the modules, together with expressions for shear at the particle's equilibrium location, for the velocity of the particle, and for the velocity dependent peak width. A sample specific module details the time dependent swelling of the two particle types to be separated. From these building blocks, the program calculates resolution as a function of the velocity of a perturbing carrier that is pumped into the system to initiate separation. Any of these modules can easily be replaced, should a more appropriate module become available.

The existing modules, with their recognized weaknesses, were used to model the resolution of an actual cell separation problem involving a wild type CHO cell and a mutant of this cell line. The two cell types were indistinguishable by any physical characteristics, but differed in terms of a membrane transport protein which allowed water to penetrate more rapidly into the mutant than into the wild type upon a reduction in ionic strength external to the cells. Due to their similarity in size, these cells were not separable by existing physical methods selective to size or mass. Although a temporary difference in size could be generated, the duration of this event was too short to allow a separation based on centrifugation or partitioning. Furthermore, cell sorting techniques based on chemical labeling of the mutated protein were also excluded, since the identity of this protein was unknown and specific labels therefore unavailable. By contrast, the sedimentation FFF in its steric/hyperlayer mode was offering a unique possibility to separate the two cell types. An earlier study had demonstrated that segregation of the two was possible using this technique. The theoretical model developed here, when tested on the experimental parameters characterizing the earlier separation, was able to predict a resolution that was in good agreement with the observed value. It should therefore prove helpful for selecting experimental conditions in future separations of a similar nature.

Acknowledgements

X.T. gratefully acknowledges support by NIH training grant GM38008-05 during part of this work; K.D.C. is similarly obliged to the NIH for support under grant GM10851-40. In addition, we wish to thank Dr. Kenneth Parker, Research In Motion Inc., Waterloo, Canada, for his help in constructing the Maple V computer program.

References

[1] X. Tong, J.F. Ash, K.D. Caldwell, J. Membr. Biol. 156 (1997) 131.
[2] R. Bettini, P.L. Catellani, P. Colombo, in: Controlled Release Society, Inc., Kyoto, Japan, 1996, p. 55.
[3] S.P. Pamomsuk, T. Hatanaka, K. Katayama, T. Koizumi, in: Controlled Release Society, Inc., Kyoto, Japan, 1996, p. 234.
[4] V.A. Prevysh, R.A. Siegel, in: Controlled Release Society, Inc., Kyoto, Japan, 1996, p. 726.
[5] G.H. Chen, A.S. Hoffman, Nature 373 (1995) 49.
[6] J.C. Giddings, Science 260 (1993) 1456.
[7] P.S. Williams, T. Koch, J.C. Giddings, Chem. Eng. Commun. 111 (1992) 121.
[8] P.S. Williams, S. Lee, J.C. Giddings, Chem. Eng. Commun. 130 (1994) 143.
[9] P.S. Williams, M.H. Moon, J.C. Giddings, Colloids Surf. A 113 (1996) 215.

[10] A.J. Goldman, R.G. Cox, H. Brenner, Chem. Eng. Sci. 22 (1967) 637.
[11] J.C. Giddings, Unified Separation Science, Wiley, New York, 1991.
[12] X. Tong, Doctoral Dissertation, University of Utah, UT, 1998.
[13] J.L. Zachary, Introduction to Scientific Programming: Computational Problem Solving Using Maple and C, A.M. Wylde, New York, 1996.
[14] G. Roy, C. Malo, J. Membr. Biol. 147 (1995) 35.
[15] G.J. Roy, J. Membr. Biol. 147 (1995) 35.
[16] X. Tong, K.D. Caldwell, J. Chromatogr. B 674 (1995) 39.